

## Ethanol blends in spark ignition engines

Wang, Chongming; Zeraati-Rezaei, Soheil; Xiang, Liming; Xu, Hongming

DOI:

[10.1016/j.apenergy.2017.01.081](https://doi.org/10.1016/j.apenergy.2017.01.081)

License:

Creative Commons: Attribution-NonCommercial-NoDerivs (CC BY-NC-ND)

*Document Version*

Peer reviewed version

*Citation for published version (Harvard):*

Wang, C, Zeraati-Rezaei, S, Xiang, L & Xu, H 2017, 'Ethanol blends in spark ignition engines: RON, octane-added value, cooling effect, compression ratio, and potential engine efficiency gain', *Applied Energy*, vol. 191, pp. 603-619. <https://doi.org/10.1016/j.apenergy.2017.01.081>

[Link to publication on Research at Birmingham portal](#)

### General rights

Unless a licence is specified above, all rights (including copyright and moral rights) in this document are retained by the authors and/or the copyright holders. The express permission of the copyright holder must be obtained for any use of this material other than for purposes permitted by law.

- Users may freely distribute the URL that is used to identify this publication.
- Users may download and/or print one copy of the publication from the University of Birmingham research portal for the purpose of private study or non-commercial research.
- User may use extracts from the document in line with the concept of 'fair dealing' under the Copyright, Designs and Patents Act 1988 (?)
- Users may not further distribute the material nor use it for the purposes of commercial gain.

Where a licence is displayed above, please note the terms and conditions of the licence govern your use of this document.

When citing, please reference the published version.

### Take down policy

While the University of Birmingham exercises care and attention in making items available there are rare occasions when an item has been uploaded in error or has been deemed to be commercially or otherwise sensitive.

If you believe that this is the case for this document, please contact [UBIRA@lists.bham.ac.uk](mailto:UBIRA@lists.bham.ac.uk) providing details and we will remove access to the work immediately and investigate.

# Splash Blended Ethanol in a Spark Ignition Engine – Effect of RON, Octane Sensitivity and Charge Cooling

Authors: <sup>1,2</sup>Wang, Chongming; <sup>2</sup>Janssen, Andreas; <sup>3</sup>Prakash, Arjun; <sup>4</sup>Cracknell, Roger; <sup>1</sup>Xu, Hongming

<sup>1</sup>. University of Birmingham, UK; <sup>2</sup>. Shell Global Solutions (Deutschland) GmbH, Germany; <sup>3</sup>. Shell Global Solutions (US), USA; <sup>4</sup>. Shell Global Solutions (UK), UK

**Abstract:** Downsized spark ignition engines have the benefit of high thermal efficiency; however, severe engine knock is a challenge. Ethanol, a renewable gasoline alternative, has a much higher octane rating and heat of vaporization than conventional gasoline, therefore, ethanol fuels are one of the options to prevent knock in downsized engines. However, the performance of ethanol blends in modern downsized engines, and the contributions of the research octane number (RON), octane sensitivity (defined as RON-MON) and charge cooling to suppressing engine knock are not fully understood. In this study, eight fuels were designed and tested, including four splash blended ethanol fuels (10 vol.%, 20 vol.%, 30 vol.% and 85 vol.% ethanol, referred to as E10, E20, E30 and E85), one match blended fuel (E0-MB) with no ethanol content but the same octane rating as E30, and three fuels (F1-F3) with different combinations of RON and octane sensitivity. The experiments were conducted in a single-cylinder direct-injection spark ignition (DISI) research engine. Load and spark timing sweep tests at 1800 rpm were carried out for E10-E85 to assess the combustion performance of these ethanol blends. In order to investigate the impact of charge cooling on combustion characteristics, the results of the load sweep for E0-MB were compared to those of E30. Load sweep tests were also carried out for F1-F3 to understand the impacts of RON and octane sensitivity on suppressing engine knock. The results showed that at the knock-limited engine loads, splash blended ethanol fuels with a higher ethanol percentage enabled higher engine thermal efficiency through allowing more advanced combustion phasing and less fuel enrichment for limiting the exhaust gas temperature under the upper limit of 850 °C, which was due to the synergic effects of higher RON and octane sensitivity, as well as better charge cooling. In comparison with octane sensitivity, RON was a more significant factor in

improving engine thermal efficiency. Charge cooling reduced engine knock tendency through lowering the unburned gas temperature.

**Keywords:** Ethanol; Direct Injection; Knocking; Charge Cooling; Octane Sensitivity

## 1. INTRODUCTION

The transportation sector is facing pressures of increased light duty mobility demand and more stringent regulations on greenhouse gas emissions [1]. Even though hybrid and electric vehicles are gaining significant popularity, conventional vehicles powered by internal combustion engines will still be the main power source for light duty transportation. Therefore, all CO<sub>2</sub> reduction techniques, including improving the efficiency of internal combustion engines, are highly relevant in the coming years.

A downsized gasoline engine is one of the proven technologies that improves engine thermal efficiency and thus reduces automotive fleet CO<sub>2</sub> emissions, by as much as 25% [2]. Downsized engines equipped with turbo- or super-chargers operate at higher engine loads to deliver the same power outputs as larger engines, thus, downsized engines lead to lower pumping losses and higher efficiency at part load operating conditions.

Ba ãa et al. [2] performed experiments on a 1.4 L downsized turbocharged engine, of which the combustion system, exhaust system and turbocharger were optimized. The 1.4 L downsized turbocharged engine had the same peak torque and power output as a 2.4 L NA-engine, but it produced a higher brake thermal efficiency. The comparative vehicle tests which were conducted using the FTP 75-cycle with pure ethanol fuel led to an 18% overall fuel consumption improvement. Judez and Sjöberg [3] investigated the downsizing possibilities of the range extender (RE) of a vehicle by making use of predictive information of the user's throttle inputs and by using a blended discharging strategy. They found that for the realistic studied example, the RE can be downsized by 30% without any performance degradation. In downsized engines, there is a trade-off between the CO<sub>2</sub> reduction and vehicle drive-ability. Bassett et al. [4] solved

the drive-ability issue by adding a 48 volt eSupercharger to a downsized 1.2 L 3-cylinder MAHLE engine. In comparison to the original downsized MAHLE engine, the new downsized engine had a faster transient response and better drive-ability characteristics, clearly demonstrating eSupercharging as a key technology for enabling further engine downsizing.

However, despite the proven advantages of downsized engines, engine knock, caused by the auto-ignition of the end gas, is one of the main challenges that stop downsized engines from achieving their full potential [5]. High octane rating fuels are one of the key solutions for suppressing engine knock [5, 6]. Ethanol, a widely used renewable gasoline alternative, has a much higher octane rating than conventional gasoline fuel. Splash blending ethanol into gasoline improves the octane rating of the resulting fuel mixture [7-10]. For example, Stein et al. [9] found that adding 10 vol.% and 20 vol.% ethanol into a RON 82 base gasoline led to 7 and 13 unit improvements of RON, respectively. The octane boost effect produced by ethanol addition is more significant for base gasoline with a lower octane rating. Additionally, ethanol has a much higher heat of vaporization (HOV) than gasoline, which offers an additional benefit of improved charge cooling when it is used in direct injection (DI) engines. Based on a study of the compression ratio (CR) distribution of engines models sold in the North American market in 2013 [11], it was found that DI engines have approximately 1 unit higher CR than PFI engines. The increase of CR in DI engines is mainly due to the cooling effect.

There are many researchers who have studied splash blended ethanol fuels in spark ignition engines and achieved promising results. For example, Jung et al. [12] studied E10, E20, and E30 fuels in a Ford 3.5 L EcoBoost DI turbocharged engine with compression ratios (CR) of 10.0:1 and 11.9:1. It was found that a 10 vol.% increase of ethanol in the blends enabled a 2 unit increase of CR without changing the knock limited combustion phase. The higher ethanol content required less fuel enrichment at high engine speeds and loads. In comparison with E10 at CR 10:1, E30 at CR 11.9:1 achieved a 7.5% CO<sub>2</sub> emission reduction when the engine was operated on the US06 Highway cycle, whilst volumetric fuel economy was approximately the same. Schwaderlapp et al. [13] investigated gasoline, match blended E20, and splash

81 blended E20 in a boosted DISI engine under full load conditions. The match blended E20 with the same  
82 RON as gasoline did not allow an increase in CR, whereas the splash blended E20 enabled a 2.2 unit  
83 increase of CR. At full engine load, due to the higher CR and the reduced fuel enrichment, the engine  
84 thermal efficiency achieved when using splash blended E20 was improved by up to 39% compared with  
85 that achieved when gasoline was used. The potential for CO<sub>2</sub> reduction by using ethanol blends was  
86 investigated using the New European Driving Cycle (NEDC) cycle over various vehicle classes ranging  
87 from mid-sized passenger cars to sport utility vehicles [13]. When the optimised CR was applied to the  
88 engine, CO<sub>2</sub> emission reductions were in the range of 3.9-4.9% for E20 in comparison with gasoline,  
89 depending on the vehicle type.

90 Apart from its high octane rating and high charge cooling effect, ethanol has a high octane sensitivity, which  
91 may play an important role in suppressing engine knock. The octane sensitivity is defined as the difference  
92 between the research octane number (RON) and motor octane number (MON), both of which are measured  
93 in cooperative fuel research (CFR) engines designed 90 years ago [14-16]. However, modern spark ignition  
94 engines, especially turbo-charged downsized engines, tend to operate at relatively lower temperatures than  
95 CFR engines, if the comparison is made with the same intake manifold pressure. This is because of the use  
96 of advanced technologies such as charge intercoolers, cooled exhaust gas recirculation (EGR) and DI [17].  
97 The RON test may partially capture ethanol's charge cooling effect, which is absent in the MON test [18].  
98 To compensate for the disconnection between the CFR engine and modern engines, an octane index (OI)  
99 was proposed as:  $OI = RON + K * (RON - MON)$  [19]. K is a scaling factor depending solely on the in-cylinder  
100 thermal and pressure history experienced by the end-gas prior to the onset of auto-ignition. The literature  
101 shows that, for some engine types at some operating conditions, a fuel with a high octane sensitivity is  
102 beneficial to reduce engine knock tendency [19-23]. For example, Remmert et al. [23] tested seven RON  
103 and MON de-correlated fuels in a prototype "Ultraboost" engine under high boost conditions, and they  
104 found that the K value tended to be negative at boosted conditions; therefore, a high octane sensitivity fuel  
105 was beneficial. Kalghatgi [24] studied 37 spark ignition engines ranging from naturally aspirated to turbo-

charged, and 1.2 to 2.4 L. It was found that under high load conditions, some engines experienced less knocking when high octane sensitivity fuels were used.

Currently, ethanol is largely used in low percentage blend forms such as E5 or E10. Higher octane splash blended ethanol fuels beyond E10 are expected to give better performance in downsized engines, however, their performance in modern downsized DISI engines, and the contributions of RON, octane sensitivity and charge cooling to combustion are not fully understood. In this study, eight fuels were designed and tested, including four splash blended ethanol (10 vol.%, 20 vol.%, 30 vol.% and 85 vol.% ethanol, noted as E10, E20, E30 and E85), one match blended fuel (E0-MB) with zero ethanol content but the same octane rating with those of E30, and three fuels (F1-F3) with different combinations of RON and octane sensitivity. The experiments were conducted in a single-cylinder DISI research engine. Load and spark timing sweep tests with an engine speed of 1800 rpm, and full load tests were carried out for E10-E85 to assess the combustion performance of ethanol blends. In order to investigate the effect of charge cooling, the load sweep was conducted for E0-MB, and the results were compared to those of E30. Load sweep tests were also carried out for F1-F3, to understand the impacts of RON and octane sensitivity on engine combustion.

## **2. EXPERIMENTAL SYSTEMS AND METHODS**

### **2.1. ENGINE AND INSTRUMENTATION**

Experiments were conducted in an AVL single-cylinder 4-stroke DISI research engine with 82 mm bore and 86 mm stroke, the setup of which is presented in Figure 1. Its combustion system features a 4-valve pent roof cylinder head equipped with variable valve timing (VVT) systems for both intake and exhaust valves. The cylinder head is equipped with a central-mounted outward opening piezo direct injector. The spark plug is located at the centre of the combustion chamber slightly tilting towards the exhaust side. The engine is coupled to an electric dynamometer, which is able to control the engine at a constant speed ( $\pm 1$  rpm) regardless of the engine power output. The engine is controlled via an IAV FI2RE management system. An AVL Indicom system is used for real time combustion indication and analysis. A Siemens CATs

system is used for signal acquisition and recording, and it communicates with the IAV FI2RE and the AVL Indicom systems. The Siemens CATs system is also used for controlling air, fuel, coolant and oil conditioning units, and the emission measurement equipment.

A Kistler pressure transducer is used for the in-cylinder pressure measurement, and it is installed in a sleeve between the intake and exhaust valves. The in-cylinder pressure is collected via a charge amplifier (ETAS ES630.1) with a resolution of 0.1 crank angles ( $^{\circ}\text{CA}$ ) between  $-30^{\circ}\text{CA}$  and  $70^{\circ}\text{CA}$  after top dead centre (ATDC), and a resolution of  $1^{\circ}\text{CA}$  at other crank angles. Some key temperature and pressure measurement locations labelled as 'T' and 'P' in Figure 1.

The engine intake system is connected to an external air handling device, capable of delivering up to 3 bar of boosted air. Air is first filtered and dried, before it is delivered to a conditioning unit. The capacity of this air conditioning unit is approximately 200 L, in which air pressure and temperature are precisely controlled using a closed-loop control system. Temperatures of fuel, coolant and oil are controlled by individual AVL conditioning systems. Fuel consumption is measured by an AVL fuel mass flow meter.

## **2.2. FUEL PROPERTIES**

Table 1 lists the properties of the fuels in this study. There are three groups of fuels in the fuel matrix. Group 1 includes E10-E85, which is for the study of engine performance of splash blended ethanol blends. E10 is a standard EN228 compliant gasoline fuel with a 10 vol.% ethanol content. E20, E30 and E85 were splash blended fuels produced by adding more ethanol into E10. Group 2 includes E0-MB and E30. E0-MB had no ethanol content, but it had the same RON and MON as E30. By comparing the engine performance of E0-MB and E30, it is possible to assess the charge cooling effect. Group 3 includes F1-F3. F1 and F2 have similar octane sensitivities but 5.6 units difference in RON, and F2 and F3 have similar RON but 5.5 units difference in octane sensitivity. Therefore, by comparing F1 and F2, and F2 and F3, it is possible to investigate the effect of RON and octane sensitivity on the engine combustion, respectively.

## 2.3. EXPERIMENTAL PROCEDURE

Table 2 lists the test matrix. For E10-E85, engine load and spark timing sweep, and full load performance tests were conducted for assessing the engine performance of splash blended ethanol fuels. In order to investigate the effect of charge cooling, RON and octane sensitivity, engine load sweep tests were conducted for E0-MB and F1-F3.

The load sweep was carried out by sweeping the intake manifold pressure from 0.65 to 2 bar at a constant engine speed of 1800 rpm. The spark timing sweep was conducted by sweeping the spark timing from KLSA-2 to KLSA+6 at a constant engine speed of 1800 rpm and a constant 1.6 bar intake manifold pressure. KLSA stands for knock limited spark advance. The engine full load was defined by IMEPs of 15 bar at 1000 rpm, 20 bar at 1800 rpm, 22 bar at 2500 rpm, 21 bar at 3500 rpm, and 20 bar at 3500 rpm.

For each fuel at a certain engine operating condition, if the engine was not knock-limited, spark timing was adjusted by aiming the combustion centre (MFB50) at  $7.5 \pm 0.5$  °aTDC, which was an approximation of the maximum brake torque (MBT) spark timing. The term ‘MFB50’ stands for the crank angle position where 50% mass fraction of the fuel has been burned. For the remainder of this paper, ‘MFB50’ and ‘combustion centre’ are used interchangeably.

When engine knock occurred, the spark timing was retarded to limit the knock intensity under the maximum tolerated intensity in order to avoid potential engine damage. In this case, spark timing is referred to as the KLSA. The same intake and exhaust valve timing, and the same injection timing maps were used for all fuels; more detailed information can be found in Appendix Table A1 and Table A2.

Table 3 lists some key engine boundary conditions. The knock intensity was defined as the maximum amplitude of in-cylinder pressure oscillation, which was obtained by filtering and rectifying the raw in-cylinder pressure data using a band-pass filter (3-30 kHz). Since the knock intensity changes significantly cycle-to-cycle, especially when engine knock occurs, in this study the mean peak knock intensity (MPKI) over 50 cycles was used as a practical indicator for knocking assessment. KLSA was determined using the MPKI listed in Table 3.



Appendix Table A3 provides some brief summary of the measurement uncertainties of key instrument.

### **3. RESULTS AND DISCUSSION**

The results and discussion has been split into two sections. In the first section, the effect of splashed blended ethanol fuels on the engine performance is presented. The benefits of using splash blended ethanol fuels in GDI engines are related to the high charge cooling effect, high RON and high octane sensitivity of ethanol, therefore, in the second section, the effect of charge cooling, and the effect of RON and octane sensitivity, are presented in order to understand their individual contribution to the engine combustion.

#### **3.1. SPLASH BLENDED ETHANOL FUELS**

Figure 2 shows the results of the engine load sweep for splash blended ethanol fuels (E10-E85) at the engine speed of 1800 rpm. Seven main combustion indicators, including the engine indicated thermal efficiency, ignition timing, combustion centre, MFB5-50, coefficient of variation (COV) of IMEP, peak in-cylinder pressure, and exhaust gas temperature, were selected to illustrate the combustion characteristics of various ethanol blends. Indicated specific fuel consumption results are also presented in Figure 2.

The spark timing was adjusted by aiming the combustion centre at  $7.5 \pm 0.5$  °aTDC if the engine was not knock-limited. At low load ( $< 8$  bar IMEP), the spark timings for all fuels were similar, whilst differences became clearer when loads higher than 12 bar IMEP were used, with higher percentage ethanol blends allowing more advanced spark timings. The onset knock-limited IMEP is approximately 8 bar for E10 and E20, 12 bar for E30, and 16 bar for E85. At 6 bar IMEP, all fuels regardless of the ethanol content had limited differences in all combustion indicators, largely because the engine was not limited by knocking, and thus the combustion phasing was optimized for each fuel. The engine thermal efficiency became differentiated as the engine was operated at knock-limited load: higher percentage ethanol blends achieved better engine indicated thermal efficiency (defined by the ratio of indicated work produced in a complete cycle and fuel energy per cycle) compared to E10. For example, in comparison with E10, E85 achieved an

approximate improvement of up to 12% in the engine indicated thermal efficiency at the IMEP ranging from 15 to 20 bar.

The early combustion duration, defined as the duration between 5-50% mass fraction burned (MFB5-50), is used to quantify the burn duration. It can be seen that higher percentage ethanol blends had shorter MFB5-50, especially at knock-limited load. MFB5-50 is presented because MFB50 was used in this study to locate the combustion centre. The MFB50 is a more reliable point to extract from the in-cylinder pressure data than MFB90 or MFB95, which were in a generally flat area of the MFB curve and as such are more susceptible to noise and cycle to cycle variation [25]. As the engine was operated at knock-limited load, faster combustion (shorter combustion duration) led to more combustion energy being transferred into effective work on the piston. The reason for the shorter combustion durations for higher percentage ethanol blends is because of 1) more advanced spark timing, and 2) faster laminar flame speed of ethanol compared to that of gasoline. The relevance of this increase in laminar flame speed to combustion in an internal combustion engine is also related to other factors, such as the mixture turbulence and the influence of the gas temperature [25].

The COV of IMEP shows the cyclic variability in indicated work per cycle. The calculation of COV of IMEP is:  $COV(IMEP) = \sigma(IMEP) / \mu(IMEP)$ , where  $\sigma(IMEP)$  is the standard deviation of IMEP, and  $\mu(IMEP)$  is the averaged IMEP in the measured cycles. Higher ethanol blends contributed to improved combustion stability, indicated by the lower COV of IMEP, especially at high load. An advanced combustion phase and shorter combustion duration both result in higher peak in-cylinder pressure. As more chemical energy released by fuel combustion was converted to effective work on the piston, the exhaust gas temperature decreased with ethanol content, especially at high load, contributing to improved engine thermal efficiency.

错误!未找到引用源。 Compared with E10, E85 led to approximately a 40% higher mass-based indicated specific fuel consumption (ISFC) at knock-free load due to its low calorific value, and the difference was reduced to 26% at the highest load, resulting from improved indicated thermal efficiency. Similarly, E20

and E30 had higher ISFC than E10 at knock-free load. As the engine load increased, the difference started to reduce or even become completely offset. Because of the higher density of ethanol than gasoline, the differences between E10 and other higher ethanol blends in volume-based ISFC could be less than these observed when considering mass-based ISFC.

Figure 3 shows the IMEP of splash blended ethanol fuels at various engine intake manifold pressures. It was observed that higher percentage ethanol blends achieved higher engine loads. Because the engine load sweep was conducted by sweeping the intake manifold pressure, it is possible to obtain IMEP data at various intake manifold pressures by interpolating the relevant data. Therefore, the IMEP results presented in Figure 3 are directly linked to the results of the combustion characteristics presented in Figure 2. It was found that higher ethanol blends achieved higher engine loads. E85 achieved 0.3 bar (3%) and 2.5 bar (14%) higher IMEP compared to E10 at 1 bar and 2 bar intake manifold pressures, respectively. This is due to more advanced spark timings, shorter combustion durations, and less exhaust energy losses of the E85 combustion compared to E10. At intake manifold pressures higher than 1.6 bar, the increase of the engine power output for E10-E30 was almost linear with ethanol content, however, as ethanol content was increased further to 85 vol.% (E85), the rate of increase in engine power output was reduced. This can be explained by the octane increase rate with various ethanol additions. The RON of E10, E20, E30 and E85 are 96.5, 99, 101.4 and 107.2, respectively. Therefore, the octane increase rate for E10-E30 is approximately 2.5 units of octane for every 10 vol.% ethanol, however, this rate was reduced to 1.1 units of octane per 10 vol.% ethanol when the ethanol content was increased from 30 vol.% to 85 vol.%. The non-linear increase of octane rating with ethanol content is a result of the synergistic effect of ethanol with alkanes in suppressing low temperature heat release. It may also be due to the RON measurement method in which the charge cooling of ethanol affects the rating [18].

Figure 4 presents the results of the spark timing sweep for splash blended ethanol fuels at 1800 rpm and 1.6 bar intake manifold pressure. At this condition, the IMEP was approximately 16 bar; the actual precise value depended on the spark timing. At this intake manifold pressure, the engine was knock limited for all

fuels. The KLSA was 1.4 °CA for E10, -2 °CA for E20, -5.7 °CA for E30, and -11.0 °CA for E85. For each fuel, the spark timing was swept in the range of KLSA-2 to KLSA+6. In the  $x$  axis of Figure 4, spark retard (spark-KLSA) represents the number of crank angle degrees that the spark timing is retarded from the KLSA of each fuel. A positive spark retard means that the spark timing is delayed from KLSA, and a negative spark retard means that spark timing is advanced from the KLSA.

The indicated thermal efficiency and IMEP shown in Figure 4 are normalized from those at the KLSA of each fuel. The normalization was done for each fuel by dividing the indicated thermal efficiency or IMEP at one spark timing by that at the KLSA. The normalization of these two parameters enabled a direct comparison of their responses/sensitivities to spark timing. It is clear that the sensitivities of indicated efficiency and IMEP to spark retard were fuel dependent. E10 was more sensitive to spark retard than other higher percentage ethanol blends. For a 2% reduction of IMEP, E10, E20, E30 and E85 allowed 1.5, 2.1, 3 and 5 °CA spark retards, respectively. The combustion centre retard showed in Figure 4 was linear to spark retard for all fuels. The rate of combustion centre retard was fuel dependent, which were 1.8, 1.6, 1.4 and 1.2 °CA per degree of spark retard for E10, E20, E30 and E85, respectively. The higher rate of combustion centre retard matched with the higher reduction rate of engine indicated thermal efficiency.

The mean peak knock intensity shown in Figure 4 indicated that for E10-E30, spark retards reduced the knock intensity, and spark timing advances from KLSA significantly increased the knock intensity, especially for E10 and E20. For E85, a low knock intensity was maintained and it was less sensitive to spark retard, showing that the CR of the engine fuelled with E85 can be further increased from 11:5:1 to improve engine thermal efficiency.

Figure 5 shows the full load results for splash blended ethanol fuels. The full load power outputs for all fuels were kept the same, as indicated by the IMEP data. The indicated thermal efficiency orders for all fuels were: E85>E30>E20>E10. Compared to E10, E20 led to 2.8-7% higher indicated thermal efficiency at full load, depending on the engine speed, whilst the improvement for E85 was in the range of 8.3-27%.

High percentage ethanol blends led to higher engine thermal efficiency due to the more advanced phase of the combustion centre, less fuel enrichment requirement and lower exhaust gas temperature. The exhaust temperature increased with engine speed due to less heat transfer. Advancing the spark timing reduces the exhaust gas temperature because the end of combustion is advanced, and more heat energy is converted into effective work on the engine piston. This explains why between 1000 and 2500 rpm engine speed, high percentage ethanol blends had lower exhaust gas temperatures. However, advancing the spark timing was restricted by engine knock. When the exhaust gas temperature exceeded the upper limit of 850 °C, fuel enrichment was used. For E85, no fuel enrichment was required at any tested engine speed, whilst E10 needed fuel enrichment from 2500 rpm engine speed.

### **3.2. EFFECTS OF RON, OCTANE SENSITIVITY AND CHARGE COOLING**

Figure 6 shows the results of the effects of RON and octane sensitivity on engine combustion. It is noteworthy that F1-F3 all contained 10 vol.% of ethanol, and their heats of vaporization were similar (see Table 1), therefore, the charge cooling effects of F1-F3 were similar. F2 had almost the same octane sensitivity as F1, but 5.6 units higher RON, therefore, by comparing the results from F1 and F2, it is possible to understand the effect of the 5.6 units difference of RON on engine combustion. From Figure 6, it is clear that at knock-limited engine load, F2 resulted in higher engine thermal efficiency, a more advanced combustion phasing, shorter combustion duration, higher in-cylinder pressure, and lower exhaust temperature. The maximum knock-free IMEP for F2 was 9.5 bar, which was approximately 3 bar higher than that of F1. Due to engine knock and pre-ignition, F1 was only tested up to 1.7 bar intake manifold pressure, whilst F2 was tested up to 2 bar intake manifold pressure. The engine knock intensity was monitored in real-time using the AVL Indicom Combustion Analyser. The knock intensity is defined as the maximum amplitude of in-cylinder pressure oscillation, which was obtained by filtering and rectifying the raw in-cylinder pressure data using a band-pass filter (3-30 kHz). The definition of a pre-ignition is when auto-ignition of the fuel/air mixture happens before the spark timing, resulting in significant engine knock

306 and very high in-cylinder pressures. The pre-ignition can be observed from the pressure trace displayed in  
307 the AVL Indicomb Combustion Analyser.

308

309 The maximum IMEP for F2 was 3.5 bar higher than that for F1, due to the higher intake manifold pressure  
310 and more advanced combustion centre. F2 also had a lower COV of IMEP at high engine load, resulting  
311 from the less retarded combustion phasing.

312 F3 had almost the same RON as F2, but 5.5 units higher octane sensitivity, therefore, by comparing results  
313 from F2 and F3, it is possible to understand the effect of 5.5 units of octane sensitivity on engine  
314 combustion. It can be seen from Figure 6 that high octane sensitivity led to improved combustion, however,  
315 its impact was much less significant than RON. F3 did not allow a higher knock-free IMEP than F2, whilst  
316 F2 led to a 3 bar higher knock-free IMEP. The maximum IMEP difference between F2 and F3 was 1.5 bar;  
317 considerably less than the 3.5 bar difference between F1 and F2. Similar evidence can also be found in the  
318 COV of IMEP, peak in-cylinder pressure and exhaust gas temperature. In addition, from Table 1 it can be  
319 seen that the increase in octane sensitivity by splash blending ethanol into E10 is less than the increase in  
320 RON. Therefore, it can be expected that, RON would contribute more to the anti-knock quality than the  
321 octane sensitivity for E10-E85.

322 In order to study the effect of charge cooling on engine combustion, E0-MB with no ethanol content but  
323 the same RON and MON as those of E30 was designed and tested. In DISI engines, apart from the octane  
324 rating of fuels, the charge cooling effect is an important contributor to suppressing engine knock. The  
325 charge cooling effect is related to the heat of vaporization; the fuel spray/droplet vaporizes after a direct  
326 injection event by absorbing heat from the compressed air within the cylinder, which reduces the in-cylinder  
327 charge temperature in proportion to the heat of vaporization of the fuel. As a result, compared to port fuel  
328 injection (PFI) engines where fuel spray is vaporized partially by absorbing heat from hot intake valves, DI  
329 engines are usually more knock resistant. Leone et al. [7] suggested that on average, DI engines had 1 unit  
330 higher CR than those of PFI engines.

The heat of vaporization of E30 and E0-MB are 551 and 365 kJ/kg, respectively. Due to the existence of 30 vol.% ethanol in E30, the lower calorific value of E30 (38.42 MJ/kg) was 8.7% lower than that of E0-MB (42.05 MJ/kg), therefore, a higher quantity of E30 was needed for the same amount of energy input than E0-MB. The collective effects of higher heat of vaporization and reduced lower calorific value resulted in E30 requiring approximately 65% more heat for vaporization at the same engine load than E0-MB.

Figure 7 shows the effect of charge cooling by comparing results from E0-MB and E30. From the indicated thermal efficiency results, it is clear that E30 was preferred at high load (>15 bar IMEP) where the engine was knock-limited. The more advanced spark timing and combustion centre, shorter combustion duration, and higher in-cylinder temperature provides strong evidence that charge cooling contributed to suppressing engine knock, even though the ethanol content was as low as 30 vol.%. In addition, E30 showed higher combustion stability, as indicated by a lower COV of IMEP. The higher engine thermal efficiency of E30 was also reflected in the lower exhaust gas temperature compared to that of E0-MB. The maximum IMEP of E30 was approximately 1.1 bar higher than that of E0-MB, resulting from the charging cooling effect. Apart from the cooling effect, the faster burning rate of ethanol is also the reason for the better combustion phasing of E30 in comparison with E0 [25].

Figure 8 shows the in-cylinder pressure and unburned zone temperature of E0-MB and E30 at 1800 rpm engine speed and 2 bar intake manifold pressure. For E30, the in-cylinder pressure rise due to combustion was more advanced than that for E0-MB, resulting from the more advanced spark timing. The peak pressure of E30 was approximately 10 bar higher than that of E0-MB. The unburned zone temperature was calculated by the AVL Concerto software. It showed that due to charge cooling, the unburned gas temperature at top dead centre (TDC) was approximately 50 K lower for E30 than that for E0-MB. The cooler unburned gas led to a longer ignition delay, therefore, E30 allowed for a 1.8 °CA more advanced spark timing at this engine operating condition.

#### 4. CONCLUSIONS

356 In this study, eight fuels were designed and tested, including four with splash blended ethanol (E10-E85),  
357 one match blended fuel (E0-MB) with zero ethanol content but the same RON and MON as those of E30,  
358 and three fuels (F1-F3) with different combinations of RON and octane sensitivity. The experiments were  
359 conducted in a single-cylinder DISI research engine. The following are conclusions drawn from the results  
360 and discussion.

361 1. Splash blended ethanol has better anti-knock properties than base gasoline, enabling a larger knock-  
362 free engine load range and more advanced combustion phasing when the engine is knock-limited. Other  
363 combustion parameters such as combustion duration, peak pressure and exhaust temperature agreed with  
364 the finding that higher ethanol blends led to better engine indicated thermal efficiency, especially at high  
365 and full load operating conditions. Compared to E10, E20 led to 2.8-7% higher indicated thermal efficiency  
366 at the full load, depending on the engine speed, whilst the improvements for E85 were in the range of 8.3-  
367 27%.

368  
369 2. Compared to E10, at knock-limited engine load, the combustion of higher percentage ethanol blends  
370 were less sensitive to spark timing retard, resulting in less negative impacts on IMEP and indicated thermal  
371 efficiency. At 1.6 bar intake pressure, advances in spark timing from KLSA caused a more severe knock  
372 intensity rise for E10 than for other higher percentage ethanol blends.

373 3. For E30, at knock limited operating conditions, the positive effect of charging cooling was reflected  
374 in the more advanced combustion phasing, higher engine thermal efficiency, and lower unburned gas  
375 temperature at TDC. The high heat of vaporization and low stoichiometric air/fuel ratio of ethanol blends  
376 both contributed to a better charge cooling effect. In addition, the faster burning rate of ethanol also  
377 contributed to this.

378 4. High RON and high octane sensitivity both contributed to improve the fuel's anti-knock quality,  
379 with the impact of RON being more significant than that of octane sensitivity. For ethanol blends, most of  
380 the anti-knock quality improvement was from the RON improvement.



381

## 382 **Acknowledgement**

383 This work was conducted at the Shell Technology Centre Hamburg. Dr. Chongming Wang was financially  
384 supported by the European Commission through the Marie Curie Program (PIAP-GA-2013-610897  
385 GENFUEL). The authors would like to thank Jakob Beutelspacher and Jan-Henrik Gross for their support  
386 in fuel blending and engine testing.

387 **Definitions, Acronyms and Abbreviations**

388

389	AFR	Air Fuel Ratio
390	ATDC	After Top Dead Centre
391	BTDC	Before Top Dead Centre
392	°CA	Crank Angle
393	CAD	Crank Angle Degree
394	CFR	Cooperative Fuel Research
395	CR	Compression Ratio
396	COV	Coefficient of Variation
397	DI	Direct Injection
398	DISI	Direct Injection Spark Ignition
399	EGR	Exhaust Gas Recirculation
400	HOV	Heat of Vaporization
401	KLSA	Knock Limited Spark Advance
402	LHV	Lower Heating Value
403	IMEP	Indicated Mean Effective Pressure
404	ISFC	Indicated Specific Fuel Consumption
405	MFB	Mass Fraction Burned
406	MPKI	Mean Peak Knock Intensity
407	MON	Motor Octane Number
408	NEDC	New European Driving Cycle
409	OI	Octane Index
410	PFI	Port Fuel Injection
411	RPM	Revolutions Per Minute
412	RON	Research Octane Number
413	SI	Spark Ignition
414	TDC	Top Dead Centre
415	VOL.%	Volumetric Percentage
416	VVT	Variable Valve Timing

## List of Figures

417

418 **Figure 1:** Engine setup

419 **Figure 2:** Results of engine load sweep for splash blended ethanol fuels

420 **Figure 3:** Engine load for splash blended ethanol fuels at various intake manifold pressures

421 **Figure 4:** Results of spark timing sweep for splash blended ethanol fuels (Note: for E85, the knock  
422 intensity was below the maximum limit in all the tested spark timing, therefore, the optimised spark timing  
423 for E85 was MBT, instead of KLSA for other fuels)

424 **Figure 5:** Full load results for splash blended ethanol fuels

425 **Figure 6:** Results for RON and octane sensitivity effect

426 **Figure 7:** Results for charge cooling effect

427 **Figure 8:** In-cylinder pressure and unburned zone temperature (calculated by AVL Concerto) of E0-  
428 MB and E30 at 1800 rpm engine speed and 2 bar intake manifold pressure

429

430

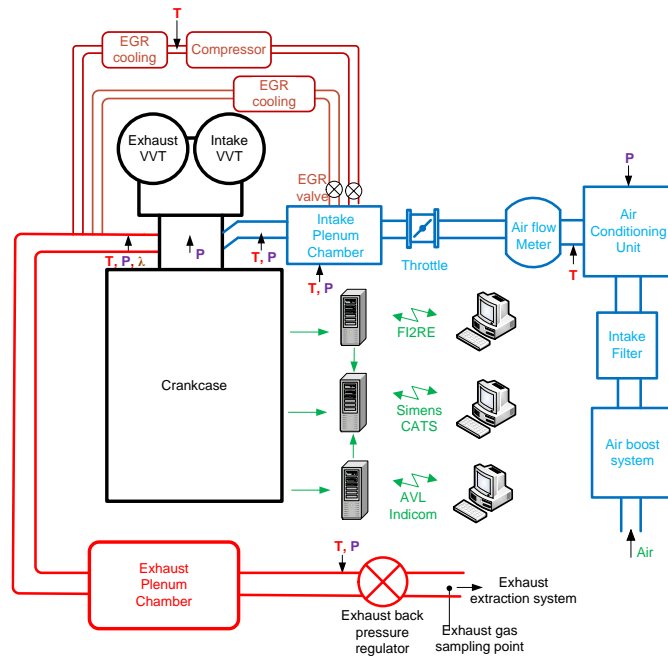


**Figure 1:** Engine setup

Results of splash blended ethanol fuels  
 Engine speed:1800 rpm; Spark timing: MBT/fixed knock intensity  
 Same valve timing and injection maps for all fuels; Lambda=1; CR=11.5:1

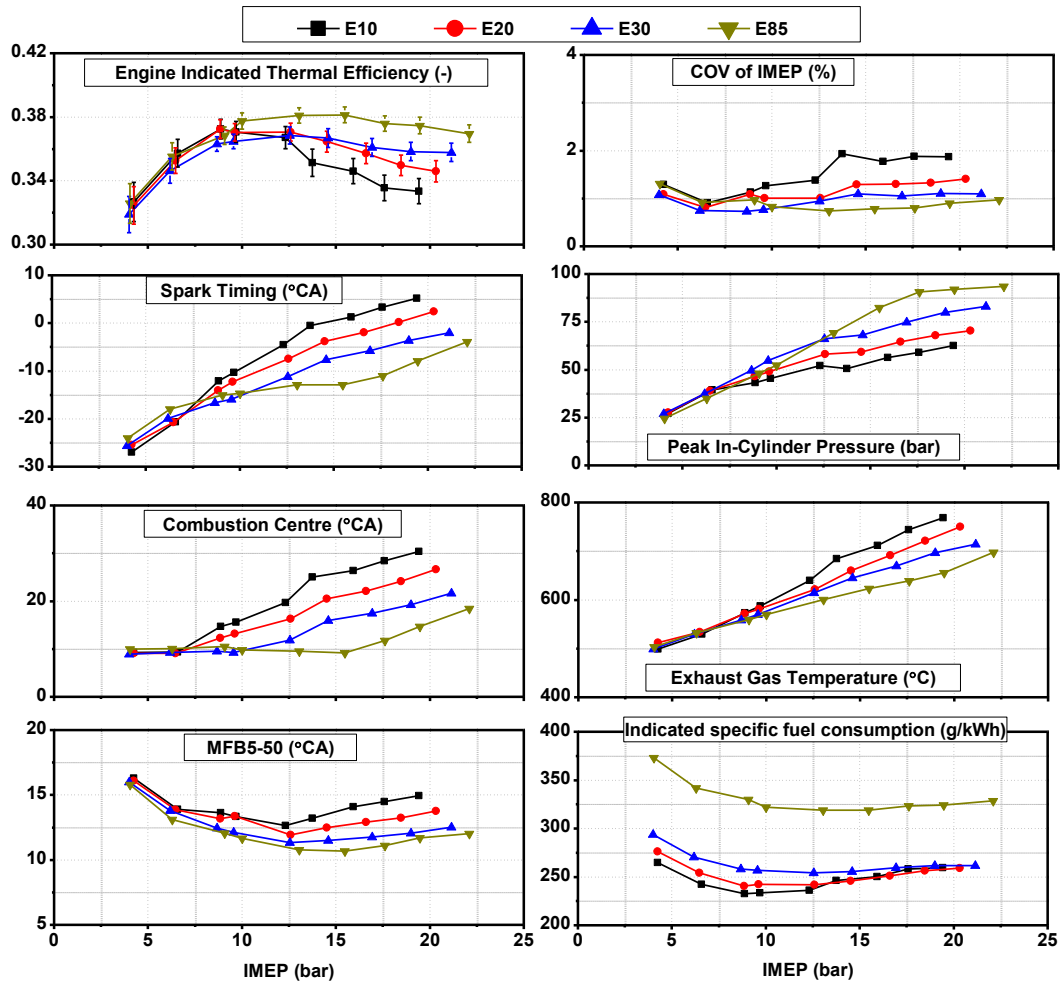


**Figure 2:** Results of engine load sweep for splash blended ethanol fuels

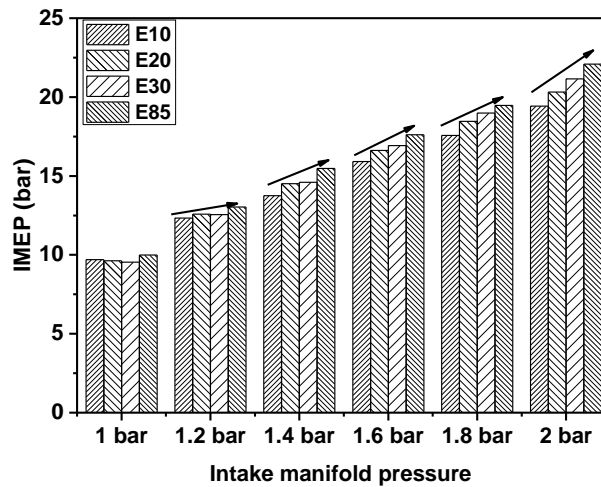


**Figure 3:** Engine load for splash blended ethanol fuels at various intake manifold pressures

### Results of spark timing sweep for splash blended ethanol fuels

Same valve timing and injection maps for all fuels; Lambda=1; CR=11.5:1

Engine speed:1800 rpm; Intake manifold pressure: 1,6 bar

KLSA: 1.4 °CA for E10; -2 °CA for E20; -5.7 °CA for E30; -11.0 °CA for E85

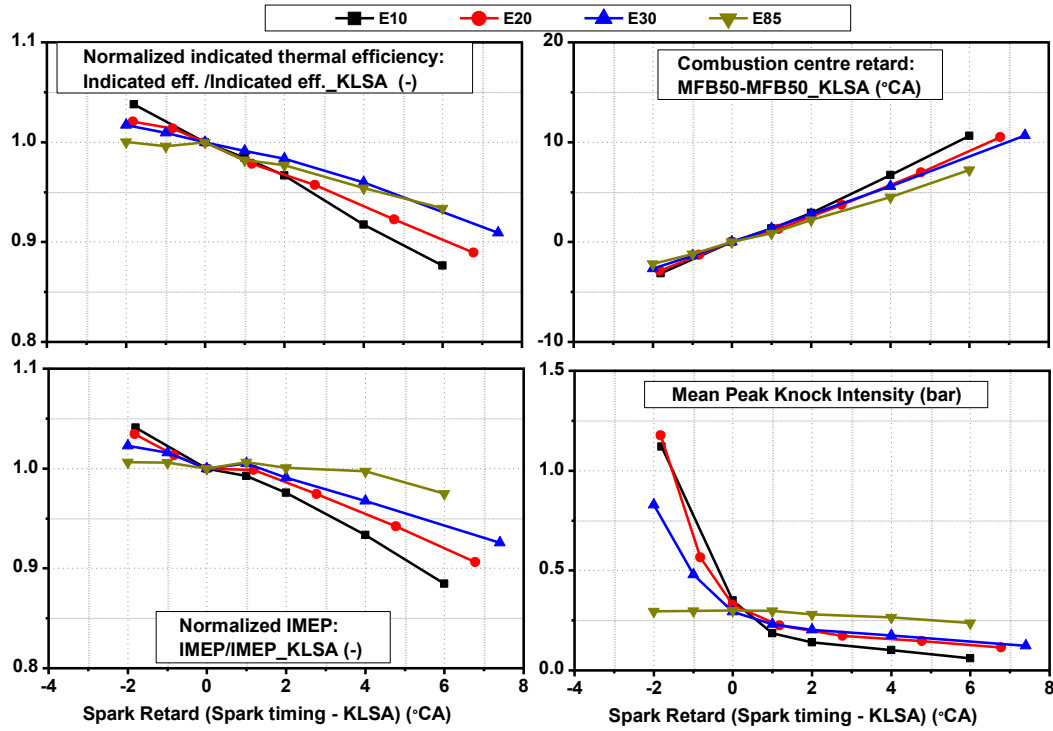


**Figure 4:** Results of spark timing sweep for splash blended ethanol fuels (Note: for E85, the knock intensity was below the maximum limit in all the tested spark timing, therefore, the optimised spark timing for E85 was MBT, instead of KLSA for other fuels)

**Results of splash blended ethanol fuels**  
 Engine speed:1000-4500 rpm; Spark timing: Fixed knock intensity  
 Same valve timing and injection timing maps for all fuels; CR=11.5:1

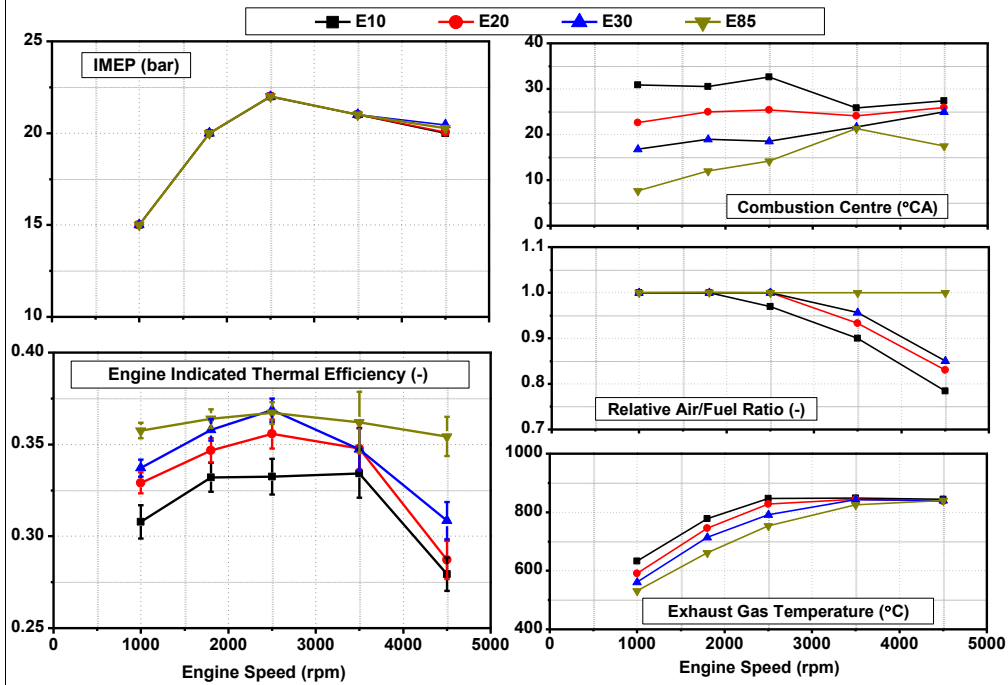


**Figure 5:** Full load results for splash blended ethanol fuels

**Effect of octane sensitivity**  
 Engine speed:1800 rpm; Spark timing: MBT/fixed knock intensity  
 Same valve timing and injection maps for all fuels; Lambda=1; CR=11.5:1

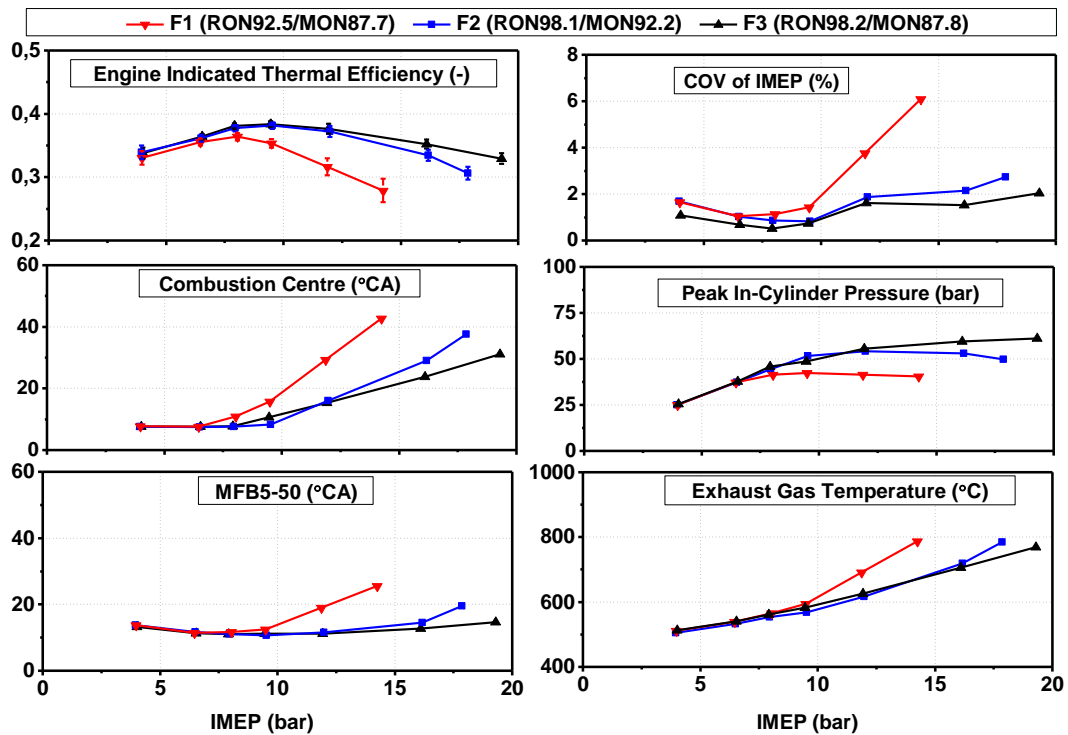


**Figure 6:** Results for RON and octane sensitivity effect

**Effect of charge cooling**  
 Engine speed:1800 rpm; Spark timing: MBT/fixed knock intensity  
 Same valve timing and injection maps for all fuels; Lambda=1; CR=11.5:1

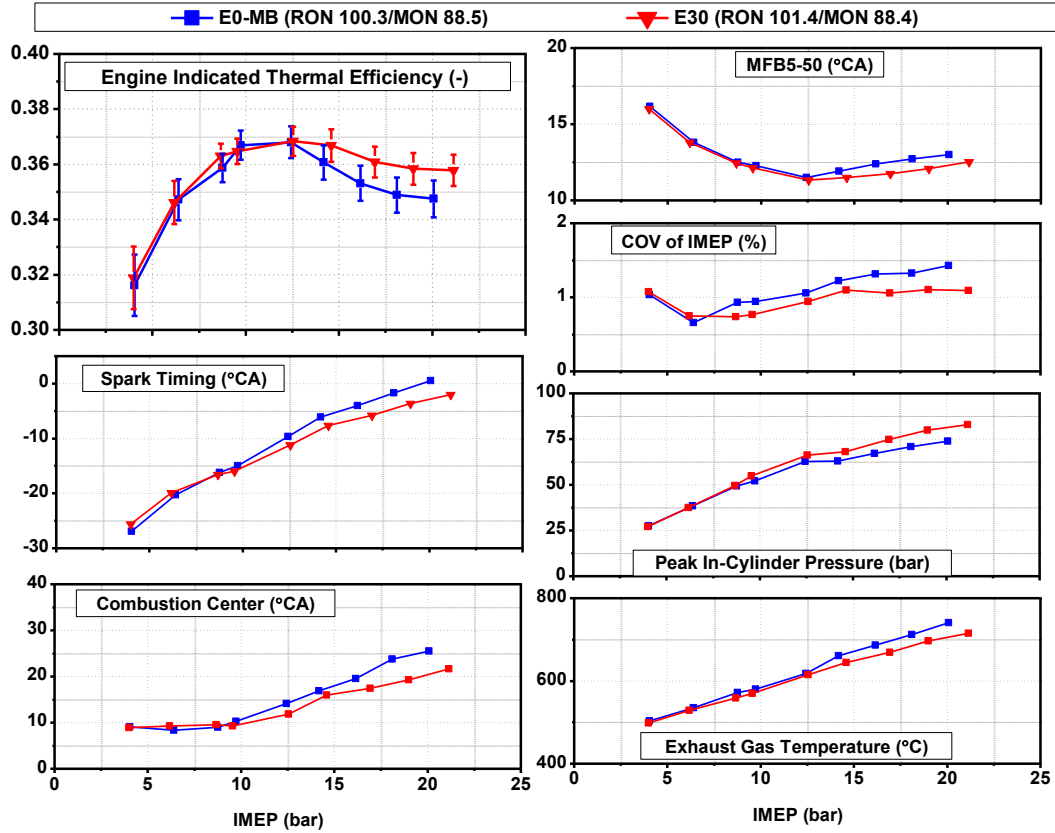


**Figure 7:** Results for charge cooling effect

**Results of Charge Cooling**  
 Engine speed:1800 rpm; Intake manifold Pres.: 2 bar Spark timing: MBT/fixed knock intensity  
 Same valve timing and injection maps for all fuels; Lambda=1; CR=11.5:1

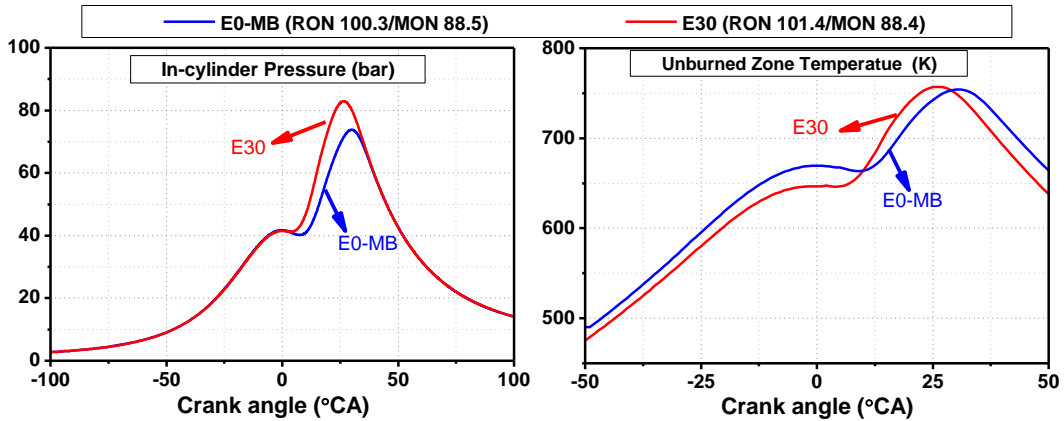


**Figure 8:** In-cylinder pressure and unburned zone temperature (calculated by AVL Concerto) of E0-MB and E30 at 1800 rpm engine speed and 2 bar intake manifold pressure



## List of Tables

459

460

461 **Table 1:** Fuel properties\*

462 **Table 2:** Test matrix

463 **Table 3:** Key engine boundary conditions

464

465 **Table 1: Fuel properties\***

		<b>E10</b>	<b>E20</b>	<b>E30</b>	<b>E85</b>	<b>E0-MB</b>	<b>F1</b>	<b>F2</b>	<b>F3</b>
<b>Ethanol</b>	vol.%	10	20	30	85	0	10	10	10
<b>RON</b>	-	96.5	99.0	101.4	107.2	100.3	92.5	98.1	98.2
<b>MON</b>	-	85.2	87.2	88.4	89.0	88.5	87.7	92.2	87.8
<b>Octane sensitivity</b>	-	11.3	11.8	13.0	18.2	11.8	4.8	5.9	10.4
<b>HOV</b>	kJ/kg_fuel	427.7	490.3	551.3	864.3	365.5	402.9	394.5	423.5
<b>HOV**</b>	kJ/kg_mixture	28.7	34.2	40.2	81.5	24.2	26.86	25.9	28.8
<b>Oxygen Content</b>	wt. %	3.7	7.5	11.2	30.6	2.2	3.92	4.0	4.5
<b>Lower Calorific Value</b>	MJ/kg	41.6	40.1	38.4	29.6	42.1	42.6	43.0	41.6
	MJ/L	30.8	30.0	28.9	23.3	31.5	30.6	30.1	30.3
<b>Stoichiometric AFR</b>	-	13.9	13.3	12.7	9.6	14.1	14.0	14.2	13.7
<b>Density</b>	kg/m <sup>3</sup>	741.7	747.2	752.9	785.8	748.4	718.0	698.6	730.0
<b>Dry Vapour Pressure Equivalent</b>	kPa	77.2	75.4	73.1	36.0	64.7	54.5	59.8	59.3
<b>Initial Boiling Point</b>	°C	30.3	30.1	30.2	49.0	28.8	35.9	35.3	35.8
<b>Final Boiling Point</b>	°C	192.2	190.8	189.2	79.2	182.6	194.2	194.8	193.4

466 \*RON and MON were measured by CFR engines; HOV was estimated by using the detailed hydrocarbon analysis results from  
467 GCMS, and a HOV library; Oxygen content was calculated from the GCMS results. Lower calorific value was calculated by  
468 using the detailed hydrocarbon analysis results from GCMS, and a lower calorific value library.

469 \*\*At stoichiometric AFR

470  
471 **Table 2: Test matrix**

	<b>Fuels</b>	<b>Engine Speed</b>	<b>Intake manifold pressure</b>	<b>Spark timing*</b>
		rpm	bar	-
Load sweep	all fuels	1800	0.65-2	MBT/KLSA
Spark timing sweep	E10-E85	1800	1.6	KLSA-2 to KLSA+6
Full load Performance	E10-E85	1000-4500	varied	KLSA

472 \* KLSA is defined by the knock limit listed in Table 3.

473  
474 **Table 3: Key engine boundary conditions**

<b>Parameter</b>	<b>unit</b>	<b>Boundary</b>
Intake air temperature	°C	34±2
Peak in-cylinder pressure	bar	≤ 130 (continuously)
Exhaust temperature	°C	≤ 840
Mean peak knock intensity (MPKI):	bar	For 1000-1800 rpm engine speed, MPKI ≤ 0.3 bar; For 2500 rpm engine speed, MPKI ≤ 0.5 bar; For 3500 rpm engine speed, MPKI ≤ 0.7 bar; For 4500 rpm engine speed, MPKI ≤ 0.9 bar;
In-cylinder pressure rise rate	bar/CAD	≤6
Relative air fuel ratio		1 or > 0.75 if fuel enrichment is needed
Exhaust back pressure	bar	1 bar at throttled conditions, and the same as the intake manifold pressure at boosted conditions

475

## Appendix

**Table A1:** Valve timing and injection strategy for load sweep test at the engine speed of 1800 rpm

Speed	IMEP	Intake valve open/close timing @ 1mm valve lift	Exhaust valve open/close timing @ 1mm valve lift	Injection timing	Injection split ratio
rpm	bar	°aTDC	°aTDC	°aTDC	-
1800	4	-12.2/179.2	-204.4/7.0	-280	-
1800	6.5	-12.2/179.2	-204.4/7.0	-280; -240	1:1
1800	8	-12.2/179.2	-204.4/7.0	-280; -240	1:1
1800	9.5	-12.2/179.2	-204.4/7.0	-280; -240	1:1
1800	12	-2.2/189.2	-214.3/-3.0	-280; -240; -200	1:1:1
1800	14	-2.2/189.2	-214.3/-3.0	-280; -240; -200	1:1:1
1800	16	12.8/204.1	-214.3/-3.0	-280; -240; -200	1:1:1
1800	18	17.8/209.1	-214.3/-3.0	-280; -240; -200	1:1:1
1800	20	17.8/209.1	-214.3/-3.0	-325; -285; -245; -205	1:1:1:1

**Table A2:** Valve timing and injection strategy for full load test

Speed	IMEP	Intake valve open/close timing @ 1mm valve lift	Exhaust valve open/close timing @ 1mm valve lift	Injection timing	Injection split ratio
rpm	bar	°aTDC	°aTDC	°aTDC	-
1000	15	12.8/204.1	-219.3/-8.0	-280; -240; -200	1:1:1
1800	20	17.8/209.1	-214.3/-3.0	-280; -240; -200	1:1:1
2500	22	22.8/214.1	-214.3/-3.0	-325; -285; -245; -205	1:1:1:1
3500	21	12.8/204.1	-214.3/-3.0	-325; -285; -245; -205; -165	1:1:1:1:1
4500	20	2.8/194.2	-214.3/-3.0	-325; -285; -245; -205; -165	1:1:1:1:1

**Table A3:** Uncertainty assessment of key instrument

Instrument	Manufacture	Model number	Measuring Range	Uncertainty
In-cylinder pressure transducer	AVL	GU22C	0 – 250 bar	±1%*
Dynamometer	HBM	T40B	-1000 – 1000 Nm	±0.01%
Fuel flow meter	AVL	735	Maximum 120 kg/h	±0.12%
Air flow meter	Elster-Instromet	Rabo G65	0 – 100 m³/h	±0.1%**
Thermocouple	Rössel Messtechnik	AL-KB-3,0-150-2	-200 – 1300 °C	±0.1 °C

\*Thermal shock error to  $\Delta P_{\max}$

\*\*Dependent on calibration tool

## References

- [1] Johnson T. Vehicular Emissions in Review. SAE Int J Engines. 2016;9:1258-75.
- [2] Bařta JGC, Pontoppidan M, Silva TRV. Exploring the limits of a down-sized ethanol direct injection spark ignited engine in different configurations in order to replace high-displacement gasoline engines. Energy Conversion and Management. 2015;105:858-71.
- [3] Judez V, Sjöberg J. Downsizing Possibilities of the Range Extender on a Range Extender Vehicle Using Predictive Information. IFAC-PapersOnLine. 2015;48:23-9.
- [4] Bassett M, Hall J, Hibberd B, Borman S, Reader S, Gray K, et al. Heavily Downsized Gasoline Demonstrator. SAE Int J Engines. 2016;9:729-38.
- [5] Jo YS, Bromberg L, Heywood J. Optimal Use of Ethanol in Dual Fuel Applications: Effects of Engine Downsizing, Spark Retard, and Compression Ratio on Fuel Economy. SAE Int J Engines. 2016;9:1087-101.
- [6] Wang CM, Xu HM, Daniel R, Ghafourian A, Herreros JM, Shuai SJ, et al. Combustion characteristics and emissions of 2-methylfuran compared to 2,5-dimethylfuran, gasoline and ethanol in a DISI engine. Fuel. 2013;103:200-11.
- [7] Leone TG, Olin ED, Anderson JE, Jung HH, Shelby MH, Stein RA. Effects of Fuel Octane Rating and Ethanol Content on Knock, Fuel Economy, and CO<sub>2</sub> for a Turbocharged DI Engine. SAE International Journal of Fuels and Lubricants. 2014;7:9-28.
- [8] Stein RA, Anderson JE, Wallington TJ. An Overview of the Effects of Ethanol-Gasoline Blends on SI Engine Performance, Fuel Efficiency, and Emissions. SAE Int J Engines. 2013;6:470-87.
- [9] Stein RA, Polovina D, Roth K, Foster M, Lynskey M, Whiting T, et al. Effect of Heat of Vaporization, Chemical Octane, and Sensitivity on Knock Limit for Ethanol - Gasoline Blends. SAE Int J Fuels Lubr. 2012;5:823-43.
- [10] Chupka GM, Christensen E, Fouts L, Alleman TL, Ratcliff M, McCormick RL. Heat of Vaporization Measurements for Ethanol Blends Up to 50 Volume Percent in Several Hydrocarbon Blendstocks and Implications for Knock in SI Engines. SAE Int J Fuels Lubr. 2015;8.
- [11] Leone TG, Anderson JE, Davis RS, Iqbal A, Reese RA, Shelby MH, et al. The Effect of Compression Ratio, Fuel Octane Rating, and Ethanol Content on Spark-Ignition Engine Efficiency. Environmental science & technology 49(18): 10778-10789.
- [12] Jung HH, Leone TG, Shelby MH, Anderson JE, Collings T. Fuel Economy and CO<sub>2</sub> Emissions of Ethanol-Gasoline Blends in a Turbocharged DI Engine. SAE Int J Engines. 2013;6:422-34.
- [13] Schwaderlapp M, Adomeit P, Kolbeck A. Ethanol and its Potential for Downsized Engine Concepts. Auto Tech Review. 2012;1:48-53.
- [14] Leppard WR. The chemical origin of fuel octane sensitivity. SAE Technical Paper 902137; 1990.
- [15] Dickinson H. The Cooperative Fuel Research and Its Results. SAE Technical Paper 290032; 1929.
- [16] Horning H. The Cooperative Fuel-Research Committee Engine. SAE Technical Paper 310019; 1931.
- [17] Davies TJ, Cracknell RF, Head B, Hobbs K, Riley T. A new method to simulate the octane appetite of any spark ignition engine. SAE Technical Paper 2011-01-1873; 2011.

523 [18] Foong TM, Morganti KJ, Brear MJ, da Silva G, Yang Y, Dryer FL. The Effect of Charge Cooling on  
524 the RON of Ethanol/Gasoline Blends. SAE Technical Paper 2013-01-0886; 2013.

525 [19] Kalghatgi G. Fuel anti-knock quality-Part I: Engine studies. SAE Technical Paper 2001-01-3584;  
526 2001.

527 [20] Kalghatgi G. Fuel/Engine Interactions: SAE International; 2014.

528 [21] Kalghatgi GT. Fuel anti-knock quality-Part II: Vehicle Studies-how relevant is Motor Octane Number  
529 (MON) in modern engines. SAE Technical Paper 2001-01-3585; 2001.

530 [22] Kalghatgi GT, Nakata K, Mogi K. Octane appetite studies in direct injection spark ignition (DISI)  
531 engines. SAE Technical Paper 2005-01-0244; 2005.

532 [23] Remmert S, Campbell S, Cracknell R, Schuetze A, Lewis A, Giles K, et al. Octane Appetite: The  
533 Relevance of a Lower Limit to the MON Specification in a Downsized, Highly Boosted DISI Engine. SAE  
534 International Journal of Fuels and Lubricants. 2014;7:743-55.

535 [24] Kalghatgi GT. Auto-ignition quality of practical fuels and implications for fuel requirements of future  
536 SI and HCCI engines. SAE Technical Paper 2005-01-0239; 2005

537 [25] Dale Turnera, Hongming Xu, Roger F Cracknellb, Vinod Natarajanc, Wyszynskia M. Combustion  
538 Performance of Bio-Ethanol at Various Blend Ratios in a Gasoline Direct Injection Engine. Fuel.  
539 2011;90:1999-2006.